THESIS

EFFECTS OF pH, TEMPERATURE AND COMPETING IONS ON THE ADSORPTION OF RADIOCESIUM ON PRUSSIAN BLUE COATED DETONATION NANODIAMONDS FROM AQUEOUS SOLUTIONS

Submitted by

Megan Zaiger

Department of

Environmental and Radiological Health Sciences

In partial fulfillment of the requirements

For the Degree of Master of Science

Colorado State University

Fort Collins, Colorado

Summer 2024

Master's Committee:

Advisor: Ralf Sudowe

Thomas Johnson

James Lindsay

ABSTRACT

EFFECTS OF pH, TEMPERATURE AND COMPETING IONS ON THE ADSORPTION OF RADIOCESIUM ON PRUSSIAN BLUE COATED DETONATION NANODIAMONDS FROM AQUEOUS SOLUTIONS

The accident at the Fukushima Nuclear Powerplant, in 2011, resulted in the generation of radioactive contaminated water which is currently being stored on site. The Tokyo Electric Power Company (TEPCO), who owns the powerplant has begun treating and releasing the water into the ocean after most of the radioactivity has been removed by the Advanced Liquid Processing System (ALPS). Currently, the techniques for preconcentration of radioisotopes, particularly radiocesium, from ocean waters are very labor and time intensive and often take months. Therefore, efficient, rapid, and reliable methods are needed for the determination of radiocesium in ocean water which represents a critical gap that this work seeks to address. A new technique using Prussian blue (PB) coated detonation nanodiamonds (DND) to adsorb radiocesium from water samples is being studied in the Sudowe Lab. The current study focuses on the effects of varying pH, temperature, competing ions, and stable cesium (Cs) on adsorption behavior. The results of the study show pH having minimal decreases in Cs adsorption, with lower adsorption as pH increases, with a lowest adsorption of 95%. Temperature changes resulted in minimal decreases in Cs adsorption with the lowest adsorption of 98% measured at 4°C. Presence of potassium chloride (KCl), sodium chloride (NaCl), and lithium chloride (LiCl) at a concentration up to 1.0 M had no effect on the uptake of radiocesium showing adsorption of

above 97% for all elements. However, adsorption decreased significantly in the presence of rubidium chloride (RbCl) as interferent concentration increased, with the lowest adsorption of 68% recorded for 1 M RbCl. The addition of stable Cs to low amounts of Cs-137 (1Bq) saw high uncertainties and low adsorption reflecting the difficulty to obtain consistent results at very low concentrations. The study has shown promise for the use of DND in environmental settings with a continued need to be able to detect low levels of Cs-137.

My research was supported by the grant T42OH009229, funded by the National Institute of Occupational Safety and Health in the Centers for Disease Control and Prevention. Its contents are solely the responsibility of the authors and do not necessarily represent the official views of the Centers for Disease Control and Prevention or the Department of Health and Human Services.

TABLE OF CONTENTS

CHAPTER 1: INTRODUCTION

1.1 Background

On March 11, 2011, a 9.0 magnitude earthquake that occurred in the Pacific Ocean, 72 km (45mi) east of the Oshika Peninsula of the Tōhoku regions shook the coast of Japan causing damage and destruction of homes and businesses. The earthquake created a 15-meter-high tsunami, which made its way to the Fukushima Prefecture destroying homes and killing thousands of people (IAEA, 2023). Over 200,000 people were evacuated when explosions occurred in the outer containment buildings enclosing the Fukushima Daiichi Nuclear Powerplant Units 1 and 3 due to a build-up of flammable hydrogen gas. A third explosion occurred in the building surrounding Unit 2. The hydrogen build-up occurred due to a lack of cooling as the tsunami impacted the backup generators and the cooling water flow at the plant. The resulting loss of electricity caused an inability to cool the reactors causing hydrogen gas to build from an exothermic reaction in the fuel cladding and later explode releasing radioactive material into the surrounding areas (IAEA, 2023).

The people who lived in the villages were not told how long they would be gone, and many did not bring any possessions as they evacuated. Thirteen years later, people are still not allowed to return to certain areas. The villages that have reopened are depleted in both resources and population as fear of the radiation still resides not only in those who had to evacuate, but also others in Japan and the rest of the world (IAEA, 2023). The Fukushima prefecture is primarily an agriculturally based area and farmers are still having difficulty selling their crops due to the continued fear of radiation.

The main concerns from reactor fuel failure are initially the short lived radioactive noble gas fission products, radioiodines and as higher fuel temperatures are achieved, radiocesium. Cs-137 (and Cs-134) is a high yield fission product (6.3%) of Uranium-235 (U-235) (NNDC, 1965). Cs-137 is of more concern due to its half-life of thirty years and complications with separation and removal from ocean water due to its high solubility in water (IAEA, 2023). Dispersion and subsequent dilution of Cs in ocean water causes difficulty in measuring low levels of Cs in a sample area (IAEA, 2023).. The lower levels of Cs-137 due to dispersion would initially seem good, the Cs-137 still remains in the environment which can be up taken by marine life and plants causing later damage. Though the radioactive material can be concentrated through evaporation methods, it takes months whereas the use of DND would take hours. TEPCO, who owns the powerplant, has removed contaminated soil or applied grout (cement) over contaminated areas nearby the reactors. The contaminated soil and water are still being stored near the powerplant as it is being decommissioned (IAEA, 2023). The contaminated water is being treated by the ALPS system, which TEPCO developed, to remove radionuclides and the treated water is currently being released slowly so that the released activity does not exceed any discharge limits (IAEA, 2023).

The IAEA set up policies and regulations to monitor the treatment and the wastewater being released, which TEPCO is following (IAEA, 2023). ALPS is a system which utilizes precipitation, adsorption, and filtration including a series of chemical reactions to remove sixty-two radionuclides; however, tritium removal is not possible (IAEA, 2023). Tritium cannot be removed as it is an isotope of hydrogen water and cannot be chemically separated. Therefore, the contaminated water is diluted with seawater before being released into the ocean to discharge limits (IAEA, 2023).

Currently, Cs-137 and Sr-90 are being removed periodically. The radioactive species are captured in filters and precipitated and the removed radionuclides are stored in high integrity containers. Discharge limits are designed to ensure that members of the public do not exceed 0.05 mSv per year. The ALPS processing area is restricted from the public access as the current area dose is 12.26 mSv/y. Japan's annual average for environmental dose per person is 2.1 mSv/y (IAEA, 2023). The IAEA has set a standard dose limit for all radionuclides in the treated water to not exceed 0.01 mSv/y. The current release dose of the treated water is expected to deliver a public dose of $2x10^{-6}$ to $4x10^{-5}$ mSv/y which is below the IAEA standards. The resulting impacts are consistent with international safety standards with all assumptions being worst case (IAEA, 2023). Despite the dose limits being below the set standard by the IAEA, there is still concern as people fear the radioactivity will harm the ocean and the countries along the coasts (IAEA, 2023).

The dose to various marine life was measured and showed a range of $2.56x10^{-4}$ to $2.92x10^{-4}$ mSv/y in flatfish, brown seaweed, and crab. The data indicated doses were below the standard of 1-10 mSv/y for flatfish and brown seaweed and 10-100 mSv/y for crab. The Cs-137 dose due to consumption of seafood for humans was calculated as $1.2x10^{-7}$ mSv/y which was also below the standard (IAEA, 2023). ALPS is able to remove radioactivity below IAEA standards; however, as mentioned in the paragraphs above, preconcentration through evaporation prior to sample measurement can take almost a months to complete, whereas the use of DND would take hours.

A need to preconcentrate Cs-137 from the water led to the creation of a new technological advancement through the use of hexacyanoferrate (iii) detonation nanodiamonds (DND) (Matsumoto et al, 2018). DND are small carbon-based molecules in a lattice like structure like a

synthetic diamond. DND are coated in Prussian Blue (PB), which is hypothesized to enhance Cs-137 adsorption to the surface of the nanodiamond.

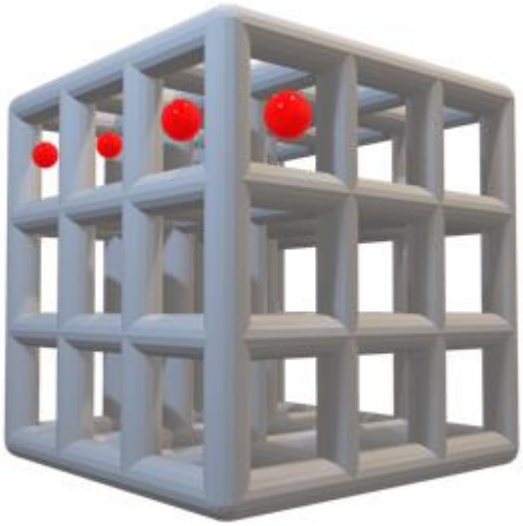

Figure 1. 3D Structure of PB with K^+ in the Lattice Voids

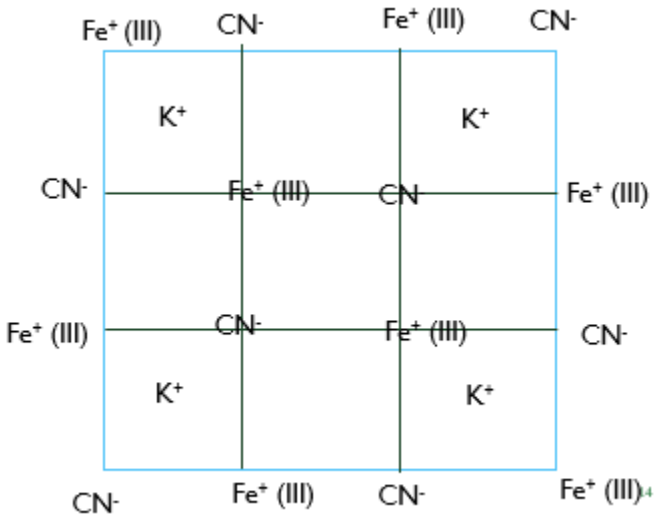

Figure 2. 2D Structure of PB with K+ in the Lattice Voids

PB is highly selective for Cs, which is exchanged with Potassium (K) in the PB. PB's structure is a lattice of iron (Fe), Cyanide (CN), Fe, CN, Fe, with K in the cubic voids which

exchanges with the Cs. Cs becomes trapped in the void after exchanging due to its larger ionic size. The 3D structure of the PB lattice as well as a 2D structure are shown in Figure 1 and 2, respectively. PB has a higher affinity for Cs, then K, then Sodium (Na) (Kharisov et al, 2010). The high affinity for Cs has been noted in past studies which saw an increase in adsorption when the nanodiamonds were coated in PB; however, there are still many unknowns that are currently being researched.

Previous PB DND studies show promise of high adsorption rates in the matter of hours. Experiments are still in the early stages examining singular factors such as pH and temperature. The research reported here will further the understanding on adsorption by expanding the range of pH to 3-9 and temperature to 4°C to 50°C. Adsorption effects from varying concentrations of competing ions KCl, NaCl, RbCl, and LiCl, and the addition of stable cesium will also be analyzed to further understand all possible environmental effects on adsorption. All experiments were counted using a High Purity Germanium (HPGe) detector which is sensitive to gamma rays. Cs-137 beta decays 100% of the time, 94.7% of the beta decays results in a metastable state of Barium-137m (Ba-137m) (NNRC, 2024). The metastable state still has residual energy in the nucleus, which is released as a gamma ray with an energy of 661.7 keV before going to the ground state of Ba-137, with an overall decay yield of 85.1%. The energy of the Ba-137m gamma ray is easily detected using an HPGe detector, which is able to pinpoint the nuclide from the photopeak. The specificity when looking at duplicate conditions is why the HPGe detector is used over other detectors.

1.2 Nanodiamonds

Nanodiamonds have a large surface area, are cost effective, do not disperse in water, and are resistant to radioactivity. Previous studies using nanocarbons for radionuclide adsorption

have shown promise which is further discussed in chapter 2. DND are synthetically created by ADÁMAS (Raileigh, North Carolina). ADÁMAS delivers the nanodiamonds in a suspension water liquid prepared for later use.

1.2 Nanodiamonds

Nanodiamonds have a large surface area, are cost effective, do not disperse in water, and are resistant to radioactivity. Previous studies using nanocarbons for radionuclide adsorption have shown promise which is further discussed in chapter 2. DND are synthetically created by ADÁMAS (Raileigh, North Carolina). ADÁMAS delivers the nanodiamonds in a suspension prepared for later use.

1.3 Ocean Water

Rain, after the Fukushima incident, further washed radioactivity into the surrounding area. Radionuclides washed into groundwater, rivers, and the ocean. Cs-137 does not bind to the water molecules but floats freely in the ocean water and is easily dispersed and washed into other areas. Clean-up measures after the incident resulted in contaminated water from the powerplant and water intrusion being placed into large storage tanks which are located at the powerplant. Storage tank water is treated by the ALPS system and released into the ocean on a scheduled basis. Ocean water is made up of many different components, particularly salts such as NaCl. The ocean pH and temperature vary throughout the world. Due to the contaminated water being treated and released into the ocean, it is important to understand the different components of ocean water and their effects on adsorption of radiocesium.

1.4 pH of Ocean Water

pH is the logarithmic measurement of the H^+ concentration in a solution. It defines the acidity or alkalinity of a solution. The lower the pH, the more acidic the solution, and the higher the number the more basic (alkaline) the solution, with a neutral solution measuring at 7.0 (Fifield, 2000). The pH of a solution is important as different speciation and complexing reactions occur at different pH values. For example, a more acidic pH of soil can kill most plants and prevent nutrients from being absorbed. However, some bacteria thrive in acidic conditions. pH values have been found to range in environmental systems throughout the world and their effects should therefore be studied when looking at environmental experimentation.

The pH of ocean water has been seen to play an important role in the chemical behavior and complexation of radioisotopes. There are many varied levels of pH in the ocean which change throughout the seasons and location. The average pH of ocean water is 8.1, which is more basic than pure water (World Ocean Review). The pH of the ocean comes from dissolved carbon dioxide (CO_2) and its interactions with the water molecules. In the ocean, the CO_2 forms bicarbonates causing the pH to be more basic. However, based on increases in carbon dioxide, the ocean has seen acidification as it went from a pH of 8.2 to 8.1 in the last century. Acidification comes from the CO_2 forming carboxylic acid instead of bicarbonate with a predicted pH of 7.8 by the year 2100 (World Ocean Review).

Acidification is an important aspect of the future of the ocean as a more acidic ocean can cause shells of mollusks to dissolve and difficulty in the formation of shells, which require carbonate to form and strengthen. The more acidic water would also cause an imbalance in marine life and a potential change in pH that can affect the ecosystem. An understanding of pH is important as pH can also affect the adsorption rate of radioisotopes as they enter the marine environment.

Japan relies on the ocean for most of its food and economy. Changes in pH of the ocean could significantly affect the adsorption of radionuclides. The large range of pH in the ocean creates a need to understand how pH affects adsorption. Therefore, it is important to consider all aspects of pH effects for both isotope adsorption and acidification of the ocean in an effort to mitigate any potential threat.

1.5 Temperature of Ocean Water

The temperature of ocean water varies throughout the world with a range of -2°C to 30°C with an average around the world of 4°C (World Ocean Review). With such a wide range of temperatures, it is important to see how temperature would effect adsorption rates of radioisotopes in order to best approach a preconcentration process. Temperatures also vary seasonally, by location, and with increases in oceans depth. Water is the densest at 4°C which could play an important role in adsorption. There are also areas of hot spots and warm vents especially around the ring of fire in which Japan is located.

The ring of fire is the name of an ecological ring of volcanoes and heat vents that cause large amounts of seismic activity. Japan is one of the countries that sits directly in the ring of fire and consequently is subject to ocean temperature changes. Therefore, understanding how various temperatures affect the adsorption rate of radioactive isotopes would enable future removal of said isotopes. It is important to study a wide range of temperatures in order to observe any possible effects on adsorption. The study would give a better understanding if a certain temperature would cause a decrease in adsorption to optimize adsorption of the radioisotopes.

1.6 Competing Ions

Cs ions have a plus one charge and binds to constituents with a negative charge. All isotopes of a given element behave in first approximation similarly, and Cs-137 is not an exception. Radioactive decay can impact chemical bonding especially if large amounts of activity are released at once and is also of concern with the thirty-year half-life of Cs-137. In order to effectively remove Cs-137 from water, its bonding properties and the behavior of any competing ions with the adsorption material must be understood. First, it is important to note that Cs behaves similarly to the elements in the same column of the periodic table including K, Na, Rb, and Li.

K particularly, is present in ocean waters and is a nutrient absorbed by fish and is utilized in the blood stream and muscle tissue (Schrand, 2009). However, Cs is a chemical analog of K and can be adsorbed in the fish instead of K, resulting in bioaccumulation at each trophic level. There are no known cases of bioaccumulation in any fauna or flora resulting in a decrease in populations, including Chornobyl (Whicker, 1981). However, to prevent possible long term impacts, the goal is to remove the Cs-137 from water via chemical interaction. However, other ions in ocean water compete for binding sites on the adsorption material causing the Cs-137 to remain as an aqueous complex in the water. Therefore, it is important to determine the potential for competition and at what concentration competition would impact the use of PB DND.

Rb, though not found in most ocean water, is important to study to better understand how Cs-137 interacts with the PB on the DND. The theory is that Cs-137 switches places with the K in the lattice voids of the PB structure. Rb is of a similar ionic size and charge energy of Cs-137 and would provide insight into the interaction with the PB. Therefore, despite Rb not being a main component of ocean water, it is important to factor in all possible competing ions to better understand the adsorption process.

CHAPTER 2: LITERATURE REVIEW

2.1 SrCoOx Nanomaterial

Strontium cobaltite (SrCoOx) is thermally treated at low temperatures (400-500° C) and has been studied for adsorption of radioisotopes (Labib et al, 2020). A facile green method was used to help in the purification and production of lanthanides from monazite. Monazite is crystalized igneous and sedimentary rock ore which was processed for the SrCoOx (Labib et al, 2020). Thorium adsorption from Monazite was studied as it is four times more abundant than Uranium for energy use and is more common in the environment thus requiring a need for separation (Labib et al, 2020). Separation techniques included: precipitation, energy chemical treatment, oxidation or reduction, ion exchange, and adsorption. Out of the methods listed, adsorption was seen to be the most cost effective to separate Thorium from the environment (Labib et al, 2020). After observing different nanomaterial studies and their effects, SrCoOx was seen to have the most potential as it has a rich and complex phase diagram, specifically topotactic phase transitions, which stores and releases large amounts of oxygen by ordering and disordering oxygen vacancies that depend on oxygen stoichiometry. Transition metal oxides in the topotactic phase transition can alter physical and chemical properties of materials making SrCoOx a good candidate for Th separation in the environment (Labib et al, 2020).

SrCoOx was used for radionuclide adsorption due to its low cost, high specific surface area, high homogeneity, high deficiency, and high purity. The use of SrCoOx and the adsorption process for the separation of Thorium from Monazite paved the way to other separation methods. Sorption in the experiment was performed in a batch process looking at pH, contact time, and metal ion concentration with two duplicate experiments (Labib et al, 2020).

The study observed pore size increases when temperature and oxygen vacancies increased. For the pH study, a gradual increase of adsorption with increase in pH was seen and thought to be due to high surface area. The time study had an increase in adsorption as time increased with a maximum adsorption at one hundred minutes. However, the removal efficiency decreased due to larger driving force transfer resistance, which increased collisions of metal ions and active sites of adsorbent but did result in a higher adsorption capacity (Labib et al, 2020).

Thorium increased with increasing pH; however, iron, that was also extracted from the monazite, decreased as pH increased. Europium depleted at a pH of 2 but had a small adsorption at a pH of 3 and larger adsorption at a pH of 4. The experiment concluded that SrCoOx was good for environmental use due to its high surface area and mobile oxygen vacancies with a promise for purification of lanthanide elements from monazite ore (Labib et al, 2020). Though the study observes Thorium separation, the understanding of nanocarbon separation through adsorption and the processes used can be applied to DND experimentation for environmental studies.

2.2 Facile Method

Graphene oxide nanoribbon aerogels (GONRs) are 3-D porous structures that were observed for the adsorption of Uranium (VI) and Thorium (IV) in an effort to overcome solid-liquid separation challenges when using powdered carbon-based nanomaterials (Yang, 2021). GONRs aerogels have a low density, good mechanical strength, large specific area, abundant oxygen containing groups, and are easily separated from water (Yang, 2021). Uranium and thorium are used as nuclear fuel to generate electricity. They are radioactive and chemically toxic in the environment. Current methods of separation include ion exchange, solvent extraction, electrochemical, membrane separation, and adsorption. Adsorption was seen to be the most effective due to economy and universality (Yang, 2021).

Graphene was used in the adsorption study due to the nanocarbon being radiation resistance, having good mechanical strength, and thermal stability (Yang, 2021). Graphene has been used in the past for wastewater treatment. However, there was difficulty with solid-liquid separations and risk of secondary pollution. Magnetic separation was proposed and used to reduce the risk of secondary pollution and increase separation. However, instability in air, acids, and bases degraded the graphene causing lower adsorption (Yang, 2021).

The decrease in adsorption led the study to observe effects on adsorption using 3-D nanomaterials due to large specific surface area and good mechanical stability, specifically GONR aerogels (Yang, 2021). The study observed the effects of pH which was kept below 4.5 to prevent hydrolysis of uranyl and thorium ions. The capacity of Uranium and Thorium increased with increasing pH and at a lower pH, active sites were taken up by Hydrogen^{+} (H^{+}) or hydronium ions (H_3O^{+}) which decreased adsorption capacity. A time study saw an increase in adsorption with an increase in contact time for the first ten minutes and equilibrium within sixty minutes. A higher correlation coefficient with pseudo -second order was also seen as well as an increase in adsorption with increasing temperature. It was concluded that the aerogel was a good material for adsorption of Uranium and Thorium (Yang, 2021). The study continues the understanding of using nanocarbons for adsorption of radionuclides in the environment and possible variations in adsorption with changes to pH, temperature, and time which further reflect in the adsorption of Cs-137 using DND.

2.3 Strontium (Sr) Removal by Microcomponents

Saccharomyces cerevisiae-Fe_3O_4 @F is a large eukaryotic fungus and single celled microorganism and was used for adsorption of Sr-90 and Strontium-89 (Sr-89) due to concern of contamination from nuclear waste management. Sr-90 and Sr-89 are considered to be the most

dangerous in and to the environment (Jundong, 2020). Isotope removal from absorbents such as sepiolite and attapulgite were observed, but had limited adsorption capacity (Jundong, 2020). Therefore, an adsorbent with a high performance was needed.

Nanomaterials have a fast reaction speed and good regeneration ability. Their superparamagnetic properties help to separate radionuclides from wastewater. Inorganic nanomaterials were used in the study; however, they tend to aggregate so their functional groups were modified (Jundong, 2020). In the study, microbial nanomaterials were used as they are easy to obtain, artificially cultivated, have many functional groups, high mass transfer efficiency, and low cost. (Jundong, 2020). After obtaining a spectra, volume, and structure, S@F was concluded to be good for an adsorbent study and a batch experiment was performed.

An adsorption increase was seen with an increase in pH value but decreased under alkaline conditions and a negative charge was observed when the pH was greater than 5.0. The study believed changes in pH caused an increase in negative charge density of S@F which caused it to favor electrostatic attraction (Jundong, 2020). A maximum adsorption was seen at a pH of 5 which was believed to be due to the high concentration OH^- in solution. An increase in concentration of Sr and an increase in adsorption capacity was observed at 300 mg/L of Sr in solution but decreased after 300 mg/L due to S@F being smaller after the specified level. They study concluded that nano-Fe3O4 particles were successful in attaching to the S@F surface and had a uniform core-shell structure; therefore, it was good for wastewater treatment (Jundong, 2020). The understanding of pH effects on adsorption is further addressed and observed in the DND study. Using the S@F results, similar observations can coincide with the same conclusions as to why pH may affect the adsorption of Cs-137 on DND.

2.4 Yittrium-90 (Y-90) sorption for nuclear medicine:

The study used DND for Y-90 adsorption due to their surface composition. DNDs have a large number of carboxyl groups on their surface which saw no oxidation effects when adsorbing Y-90. The study observed targeted delivery of biocompatible and versatile functionalization surface of Y-90 sorption with powder form DND (Babenya, 2021). Y-90 and Sr-90 are in secular equilibrium, production rate of Y-90 equals the decay rate of Sr-90 (Babenya, 2021). Therefore, the Y-90 needed separation from Sr-90 through the use of extraction chromatography using RE resin with a resulting 0.2% retention on the DND (Babenya, 2021).

A sorption and desorption study were then conducted with a pH of 7.3 in a Prussian Blue Solution (PBS). The DND in the solution saw changes in oxygen and carbon but not in nitrogen. A pH range from 5-7 was studied and saw no differences in sorption as well as no change in structure when in acids (Babenya, 2021). Desorption values did not change over time. A decrease in aggregate size from 600 to 80 nm saw an increase in sorption by 15% and decrease in desorption by 5%. In conclusion, nanodiamonds were a good use of sorption and desorption of Y-90 and could be used in nuclear medicine (Babenya, 2021). The study showed an increase in adsorption using Prussian blue coated DND. Therefore, the use of PB coated DND were used in the Cs-137 study to help improve adsorption out of aqueous solutions.

2.5 Uranium Removal via Citrus Peel (Lemon)

Cerium Oxide was extracted from citrus lemon peels using a green synthesis route with ammonium cerium nitrate as the prime precursor. It was proposed that the extract would have a spherical morphology. The main goal of the study was to remove U (VI) ions from polluted water (Komal, 2021). The experiment used cerium oxide from lemon peel extract which had never been reported on before. The reasoning was to use an organic material that was cost effective and readily available (Komal, 2021).

A near spherical shape was observed of the nanoparticles. The adsorption capacity of U (VI) increased with increases in cerium oxide adsorbent dosage with a maximum adsorption at 0.003 mg. However, an increase in adsorbent concentration resulted in a decrease of U (VI) ion adsorption (Komal, 2021). Overall, the use of the citrus lemon peel was seen to be a success in biosynthesis through simple, low cost, and environmentally friendly green process (Komal, 2021). The isotherms were well matched to the experimental results. The study further showed the importance of a environmentally friendly and cost effective method to adsorb radionuclides from the environment. DND was selected for Cs-137 adsorption in aqueous solutions using the same parameters in the study.

2.6 Biomass Absorption of Uranium (U)

Biomass adsorption of U is cost effective with high removal rates and high selectivity for low metal concentrations. The study looked at plant-based nanomaterials such as: grain, cash crops, and pine residues (Meiqing, 2021). U in the body can cause an increase in white blood cells and cancer as well as other lesions. In the environment it can harm growth and reproduction of marine life. Adsorption techniques were used as it is low cost, has easy industrialization, and simple preparation (Meiqing, 2021).

The plant-based nanomaterials showed a strong affinity toward organic molecules and oxygen containing surface functional groups. Other biomass carbons used had good thermal stability, a rigid porous structure, and good mechanical strength (Meiqing, 2021). However, each plant material studied showed adsorption potential but not as high as other carbon nanoparticles seen in other studies. Chitosan showed the most potential but dispersed in aqueous solutions. The study concluded that plant-based and biomass carbon were not good for environmental adsorption of U (Meiqing, 2021). DND do not disperse in water and are just as cost effective as

using the plant-based and biomass carbon nanomaterials. The research helped pave the way for future studies using other nanocarbons by factoring out plant-based and biomass carbon uses for radionuclide separations.

2.7 Amine Graphene

The paper looked at amine functionalized graphene oxide/zinc hexacyanoferrate and their morphologies, large specific surface areas, pore sizes, functional groups, and thermal stabilities. The experiment used Graphene oxide (GO) powder as it has a large specific surface area and 2-D structure. It also has a high affinity as an adsorbent and can remove Cs^{+}., sodium bisulfite solution, zinc chloride, ammonia, and isopropyl alcohol (Jung-Weon, 2020). The GO adsorbent saw a lower capacity with a maximum value of 1 mmol/g. The removal efficiency was low for low and high pH ranges and highest at pH 5. The efficiency did decrease from pH 5 to pH 11 which may be due to a decrease in HCF stability under high alkaline conditions due to breaking of bonds (Jung-Weon, 2020). Low removal efficiency under acidic conditions was seen to be due to competition with Cs^{+} and H^{+} as H^{+} was seen to have a higher concentration. The adsorption reaction was seen to be dependent on contact time which fit well with the Temkin and Freundlich models (Jung-Weon, 2020). Based on the study, graphene nanoparticles were considered good when treating low level wastewater. The experiments performed in the study were built upon using DND to further understand Cs-137 adsorption in the environment when factoring in pH, temperature, and competing ions.

CHAPTER 3: MATERIALS AND METHODS

3.1 Materials

The following materials were used:

- 0.05 M $K_4[Fe(CN)_6]$ (Potassium ferricyanide) (Sigma-Aldrich ACS Reagent Grade)
- 0.1 M $CuCl_2$ (Copper (II) chloride) (Sigma-Aldrich EN Grade)
- KCl (Potassium Chloride) (VWR Life Sciences ACS Grade)
- KH_2PO_4 (Potassium Phosphate Monobasic) (Fischer Chemical Certified ACS)
- LiCl (Lithium Chloride) (Sigma-Aldrich ACS Reagent Grade)
- Na_2CO_3 (Sodium Carbonate) (Sigma-Aldrich ACS Reagent Grade)
- NaCl (Sodium Chloride) Fischer Chemical Certified ACS Grade
- $NaHCO_3$ (Sodium Bicarbonate) (Fisher Chemical Certified ACS Grade)
- NaOH (Sodium hydroxide) (Sigma-Aldrich ACS Reagent Grade)
- Sigma-Aldrich Reagent Plus Grade RbCl (Rubidium Chloride)
- Cesium, Single Element ICP/MS Certified Reference Standard, 10 μg/mL
- 30 nm nanodimaonds (ADÁMAS).

- 1000 Bq/mL Cs-137 working solution
- 15 mL centrifuge tubes
- 50 mL Nalgene plastic jars
- Automatic pH meter
- Automatic pipettors
- Automatic shaker

- Centrifuge
- Tube racks
- Ultra-pure water (18.2 MΩ)
- HPGe detectors (Meitner 35% relative efficiency, Strassmann & Hahn 65% relative efficiency)

3.2 Methods

3.2.1 Pretreatment of Detonation Nanodiamonds:

Detonation nanodiamonds with a particle size of thirty nanometer (nm) were purchased from ADÁMAS (Raleigh, North Carolina). The DND were stored in water in a 1% weight by weight (w/w) solution, of which 30 mL was pipetted into a porcelain ceramic crucible. The DND were then dried in a Thermolyne Furnace at 100°C until the storage solution had completely evaporated. The dried nannodiamonds can be seen in Figure 3.

Figure 1. Dried DND

Using the same furnace, the temperature was then increased to 400°C for eight hours in order to oxidize the surface of the DND. Oxidation of the surface allows for the PB coating to adhere

better to the surface of the DND. The nanodiamonds were subsequently diluted back a 1% w/w solution using ultra-pure water.

3.2.2 Adsorbent Preparation:

The Prussian Blue adsorbent was prepared in batches. At the start, the storage solution was ultrasonicated for thirty minutes to ensure a homogeneous suspension of the nanodiamonds (Deak, 2021). Each batch included 0.4 mL of 1% w/w nanodiamond solution, which was added to 40 mL of DI water. The solution was stirred for one minute. A measure of 0.4 mL of 0.1 M $CuCl_2$ was then added to the solution and stirred for five minutes. Finally, 0.4 mL of 0.05 M $K_4[Fe(CN)_6]$ was added to the solution and stirred for one hour. The suspension was left to settle overnight, and the excess supernatant was pipetted off. The remaining solution was then poured into multiple petri dishes and left to air dry (Deak, 2021). The dried coated nanodiamonds were then put into labeled centrifuge tubes for later use (Figure 4). The steps were repeated until all batches of nanodiamonds were coated.

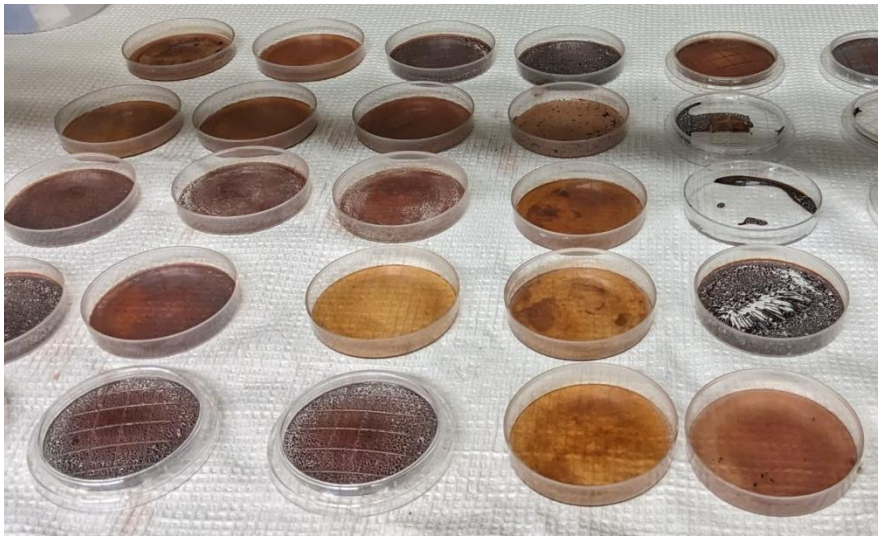

Figure 2. Dried PB coated DND

3.2.3 pH Procedure:

Buffer solutions were prepared for pH 3.0 and pH 3.5 using oxalic acid ($C_6H_6O_7$) and sodium bicarbonate ($NaHCO_3$), while pH 4.0, 4.5, 5.0, 5.5, 6.0, 7.0, 7.5, 8.0, 8.5, and 9.0 used KH_2PO_4 and sodium hydroxide (NaOH). Calcium chloride ($CaCl_2$) and DI water was used to adjust the pH to 6.5. All buffer solutions were measured using an automatic pH meter. Each pH buffer solution was labeled and put in its own glass storage jar for later use.

Three 15 mL centrifuge tubes were used for each pH buffer solution, 3 for pH 3.0, 3 for pH 3.5, etc. Each tube contained 15 mg of the 30 nm nanodiamonds and 9.9 mL of the correct pH adjusted DI water to each tube. Next, each tube was spiked with 0.1 mL of Cs-137 working solution. All tubes were shaken for six hours and left to sit overnight to optimize contact time. The next day, each sample was centrifuged for ten minutes at 3000 rpm. The supernatant was then poured into a 50 mL Nalgene jar, which was subsequently each counted for six hours on an HPGe detector. The spectra were compared to a standard consisting of 9.9 mL of DI water and 0.1 mL of Cs-137 working solution sample without DND in the same type of 50 mL Nalgene jar.

3.2.4 Temperature procedure

Deionized water was used as a solution for the temperature study and samples were shaken for six hours at various temperatures. Experiments were carried out in triplicate at each 4°C, 10°C, 15°C, 20°C, 25°C, 30°C, 35°C, 40°C, 45°C, and 50°C. Fifteen mg (0.015 g) of the 30 nm nanodiamonds were added to each 15 mL centrifuge tubes together with 9.9 mL of DI water and 0.1 mL of the Cs-137 working solution. The three tubes for each temperature were agitated at the stated temperature for six hours using a temperature-controlled shaker and then left overnight at room temperature. The next day, each sample was centrifuged at 3000 rpm for ten minutes. The

supernatant was then poured into separate 50 mL Nalgene bottles and counted on an HPGe detector. The spectra were then compared to a standard consisting of 9.9 mL of DI water and 0.1 mL of the Cs-137 working solution without DND.

3.2.5 Competing Ion Procedure

The solutions for the competing ion procedure were all prepared in the same manner. The appropriate amounts of LiCl, NaCl, KCl, and RbCl salts for each concentration were weighed out in grams and added to 30 mL of DI water. The salt was dissolved and set aside for the experiment. For each interfering ion, solutions with concentrations ranging from 0.001 M to 1.0 M were prepared with 15 mg of DND and 9.9 mL of the appropriate concentration of the interferents. Each sample was spiked with 0.1 mL of Cs-137 working solution and shaken for six hours. They were left to sit overnight before being centrifuged at 3000 rpm for ten minutes. The supernatant was then poured into a 50 mL Nalgene jar and counted on an HPGe detector and compared to the comparison standard mentioned above.

3.2.6 Stable Cs Procedure

Various amounts of a solution containing 10 μg/mL of stable Cs were added to a range of DI water. The stable Cs added ranged from 0.01 μg to 10 μg and the DI water from 8.999 mL to 9.999 mL. Three centrifuge tubes were labeled for each amount of stable Cs and 15 mg of DND was added to each vial. The calculated amount of DI water was then added to each appropriate tube. Each vial was then spiked with 0.001 mL of Cs-137 working solution. Each tube was shaken for six hours and then left to sit overnight. They were then centrifuged at 3000 rpm for ten minutes. The supernatant was poured into a correctly labeled 50 mL Nalgene jar which was

counted on an HPGe. The results were compared to a jar that contained no DND, 9.999 mL of DI water, and 0.001 mL of Cs-137 working solution.

CHAPTER 4: RESULTS

4.1: pH study

The pH study examined how varying pH buffer solutions affect the adsorption of Cs to nanodiamonds. A pH range of 3.0 to 9.0 was observed and analyzed on an HPGe detector. The results show high adsorption for lower pH values at approximately 99% adsorption. Lower adsorption was seen for higher pH values with the lowest adsorption at a pH of 6.5 of around 95%. No adsorption fell below 95% demonstrating overall effectiveness of nanodiamond adsorption with varying pH.

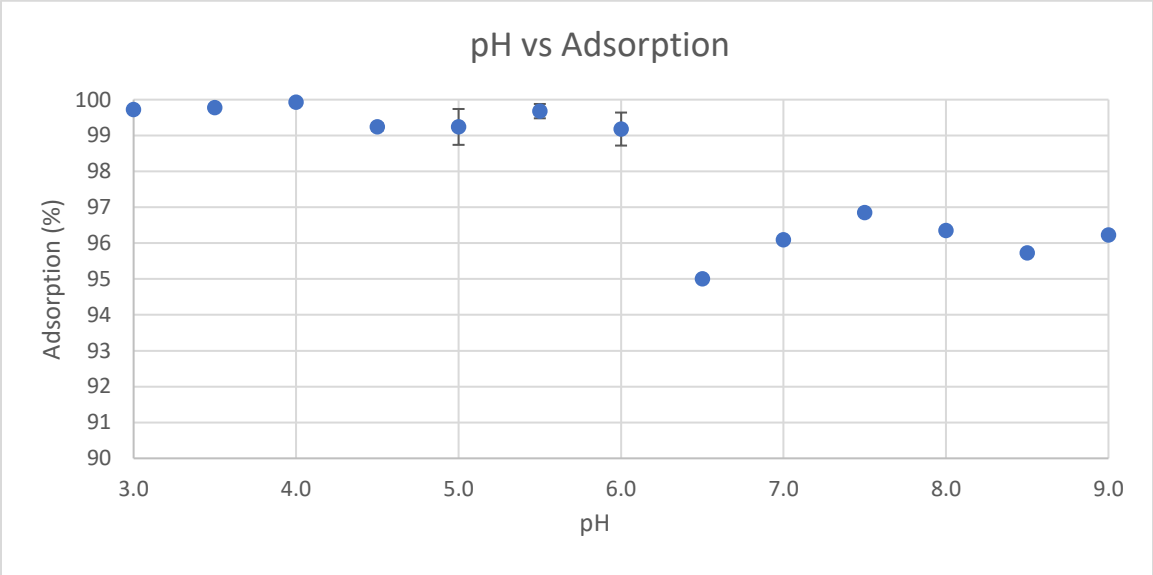

Figure 5. Percent adsorption of radiocesium for the pH range of 3.0 to 9.0.

4.2: Temperature Study

The temperature study included a range of 4°C to 50°C. All data points had the same geometry of 10 mL with 9.9 mL of DI water and 0.1 mL (100 Bq) of Cs-137 working solution.

Adsorption fluctuated with most temperature near 99%. The lowest adsorption was at 4° C at 98%. Overall, adsorption does not seem to decrease enough with varying temperatures.

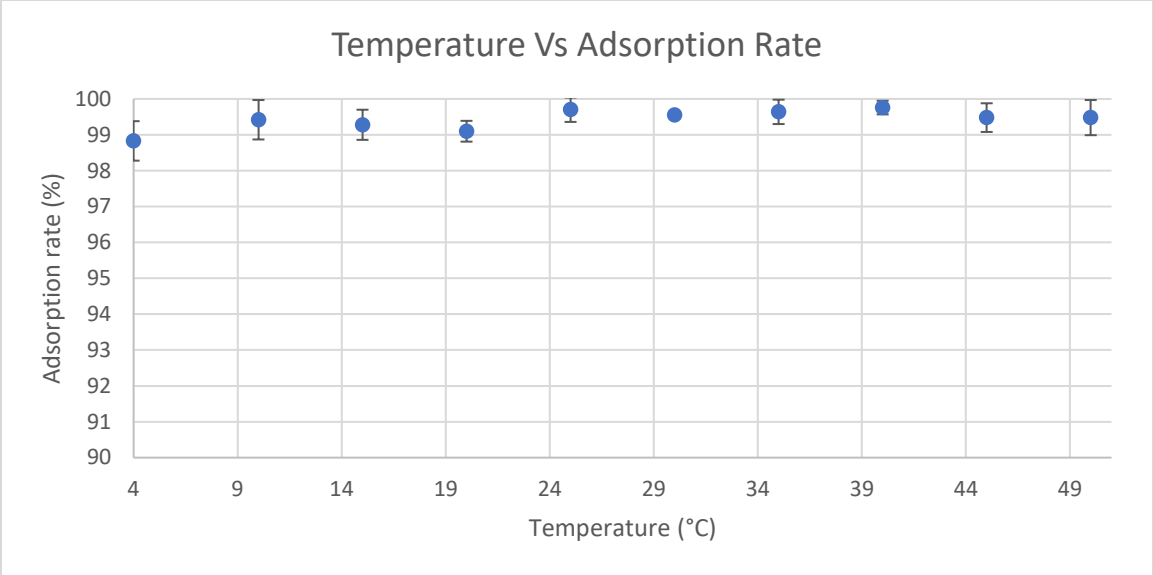

Figure 6. Percent adsorption of radiocesium for temperature ranges of 4°C to 50°C.

4.3 KCl Study

A range of 0.001 M to 1.0 M concentration of KCl was studied. There is an increase in adsorption of around 1% from 0.1 M to 0.25 M which is seen in all of the salt samples. Adsorption decreased as concentration of the KCl salt solution increased with the lowest adsorption occurring at the 1.0 M concentration at ~ 98%.

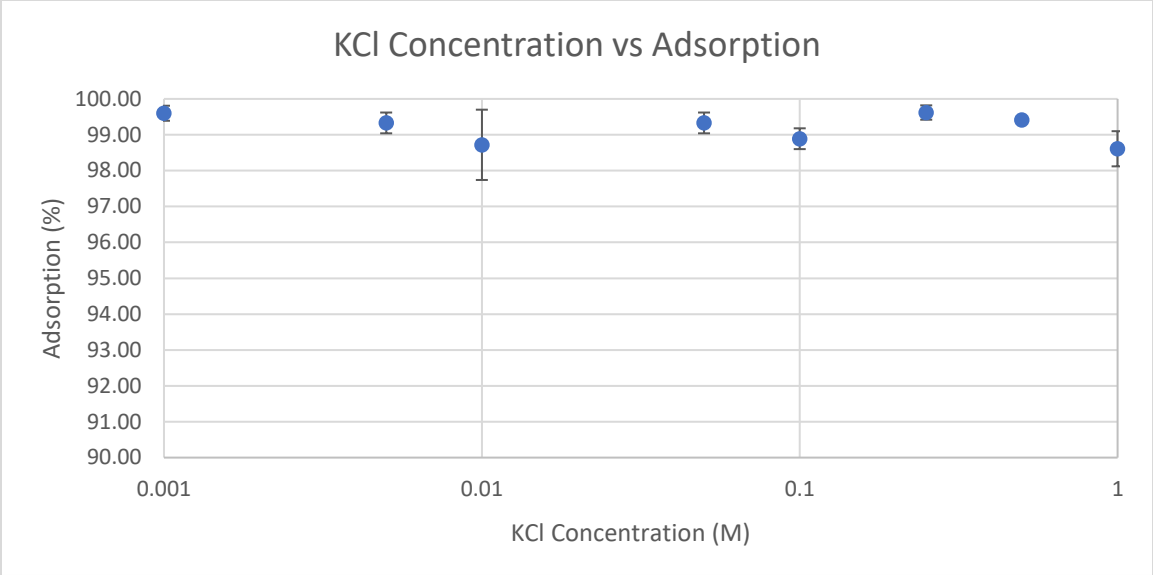

Figure 7. Percent adsorption of radiocesium as a function of KCl concentration.

4.4 NaCl Study

The NaCl study looked at a concentration from 0.001 M to 1.0 M. There is a slight increase in adsorption of around 1% from 0.1 M to 0.25 M which was seen in all the salt samples. Despite the increase, all but the 0.1 M concentration was above 99%. The lowest adsorption was at the 0.1 M concentration which remained above an adsorption of 98%.

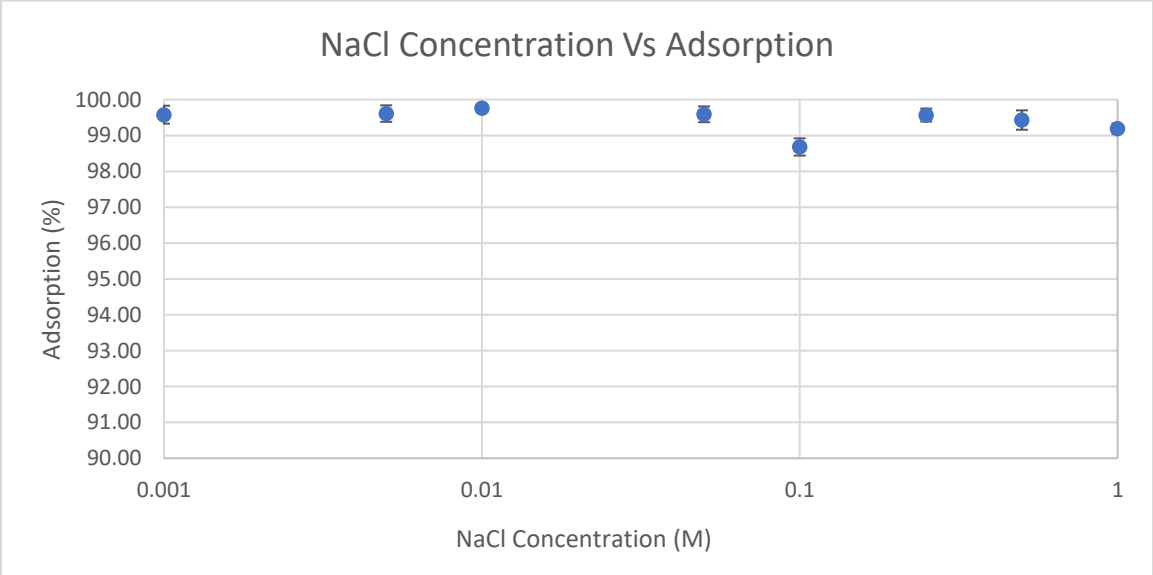

Figure 8. Percent adsorption of radiocesium as a function of NaCl concentration.

4.5 RbCl Study

The RbCl study shows a range from 0.001 M to 1.0 M concentration. There is an increase in adsorption of around 3% between 0.1 M and 0.25 M as stated in the other salt samples. Adsorption decreased as RbCl concentration increased with the lowest adsorption at the 1.0 M concentration of ~ 68%. The lower adsorption for RbCl compared to the other salt solutions will be discussed in the following chapter.

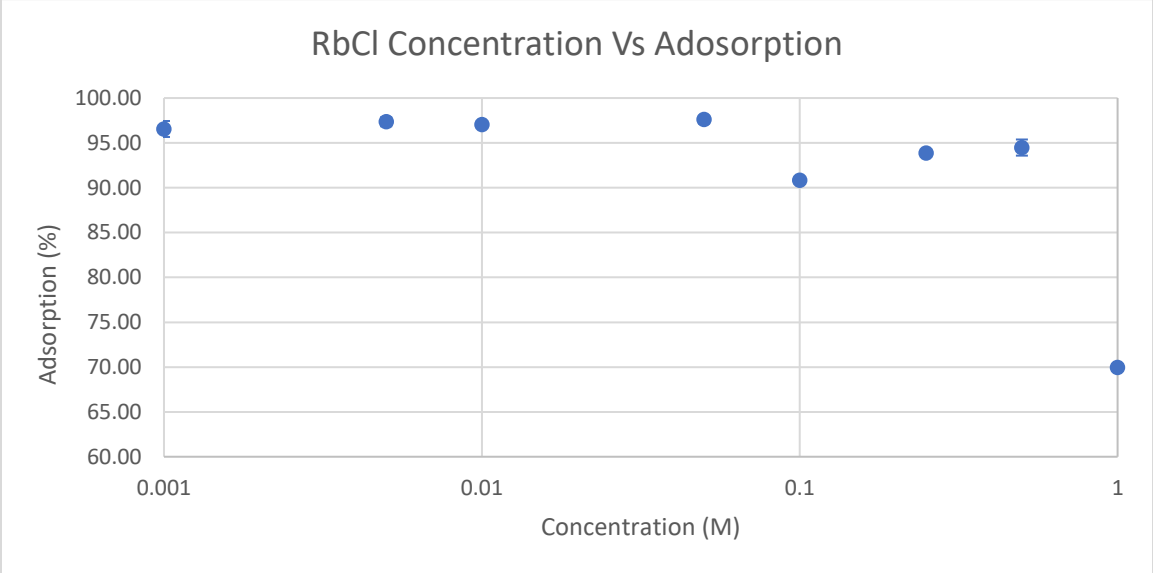

Figure 9. Percent adsorption of radiocesium as a function of RbCl concentration.

4.6 LiCl Study

The LiCl was studied for a range of 0.001 M to 1.0 M concentrations. Fluctuations are seen in the data are similar to all salt samples. Adsorption decreased as LiCl concentration increased with the lowest adsorption at 1.0 M concentration of ~97%.

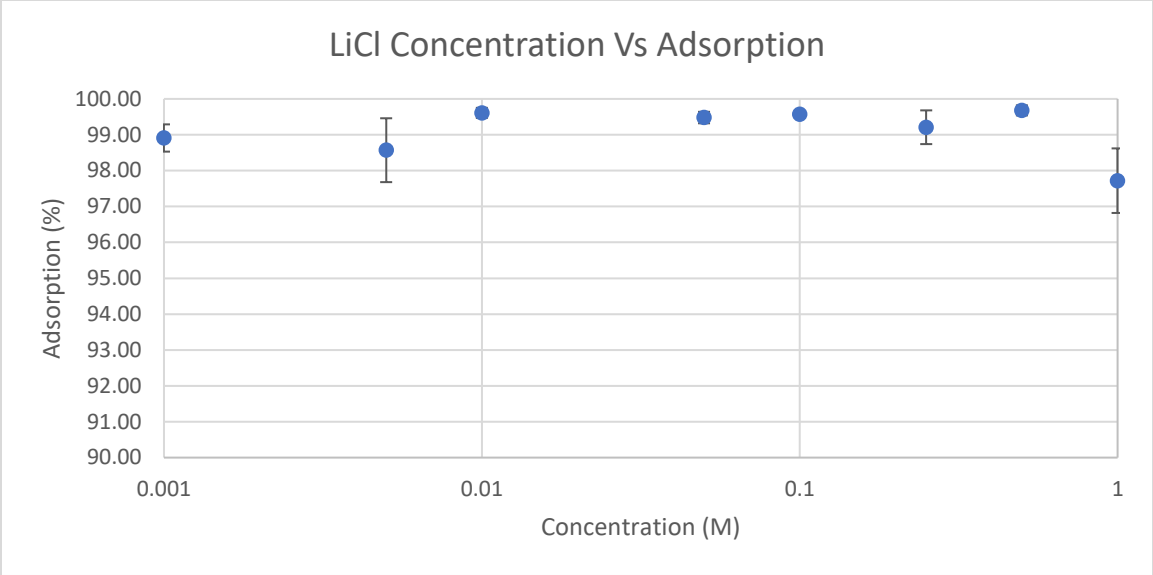

Figure 10. Percent adsorption of radiocesium as a function of LiCl concentration.

4.7 Stable Cs Study

The stable Cs study looked at a range of 0.01 µg per 9.999 mL of DI to 10 µg per 8.999 mL of DI water Adsorptions with the study varied greatly from 61% to 137% with large uncertainties. The discussion of the possibility of the results will be discussed in the next chapter.

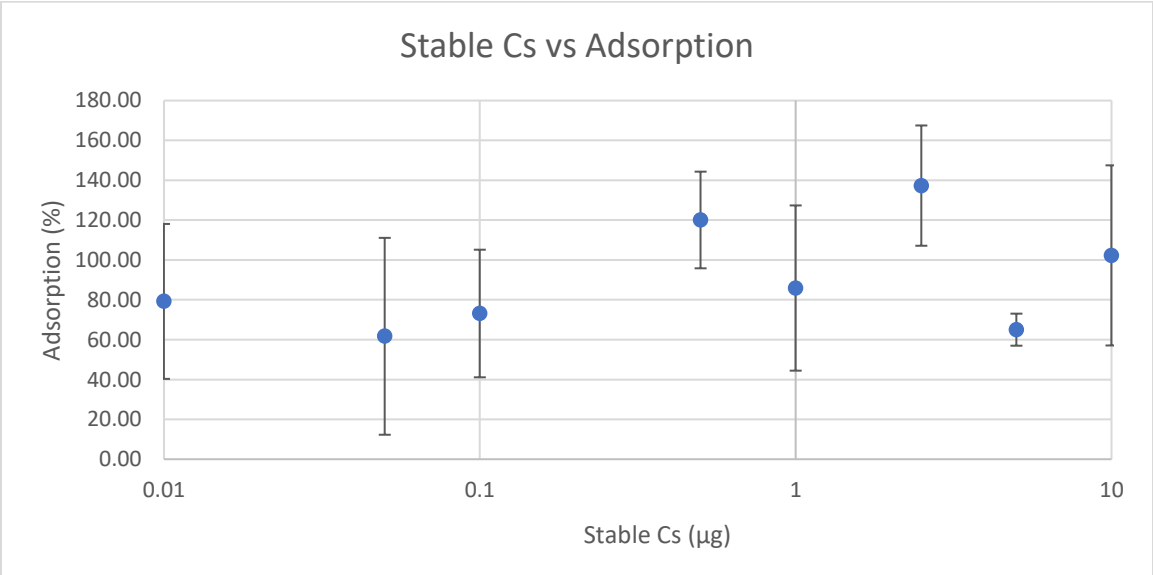

Figure 11. Adsorption of 1 Bq Cs-137 as a function of added stable cesium carrier.

CHAPTER 5: DISCUSSION

5.1 pH Study

The pH study range was 3.0 to 9.0 in order to better understand the effects of acidic and basic solutions on adsorption of Cs-137 from aqueous solutions. A decrease in adsorption was seen for higher pH value adjusted samples, starting at a pH of 6.5. The lowest adsorption occurred at a pH of 6.5 with a value of ~ 97%. Adsorption at lower pH values were all near 99% and did not fall below said percentage. The decrease in adsorption for higher pH values is important to understand when looking at environmental experimentation. The environment varies in pH around the world in both soil and water with an average ocean pH of 8.1. It is important to understand the interactions pH has with Cs-137 adsorption if the experiment is to be used in the environment. The decrease seen in higher pH values is consistent with past studies and was further pronounced in the study with a larger range of acidic and basic solutions. The decrease at higher pH values may be due to the surface properties of the DND in basic solutions. The surface of DND can be positively charged or negatively charged. The basic solutions could be causing a switch in the charge towards more neutral which would explain the decrease in adsorption.

5.2 Temperature Study

The range of temperatures investigated in the study was from 4°C to 50°C. Temperatures vary in the ocean with the densest ocean water at 4°C. As water cools, the water molecules become more rigid with ice forming a lattice structure. The structural rigidity of the water as it cools makes adsorption out of water difficult as the Cs could adhere to lattice voids. The study saw adsorption rates above 98% with the majority above 99%. At 4°C, adsorption dropped to around 98% which is consistent with the density of the water at 4°C forming lattice structures.

The Cs could be becoming trapped in the lattice voids of structural rigid water molecules similarly to how Cs becomes stuck in the PB lattice voids. Understanding the density of the water and how the molecules interact is important for environmental studies. Based on the results seen in the study, Cs-137 preconcentration from water in the ocean will not be greatly affected to a large degree with changes in temperature.

5.3 KCl Study

K is a chemical analog for Cs and both are Group 1A elements. Both ions bond and are utilized as analogs in the body. Both K and Cs are utilized as nutrients, entering the blood stream and utilized in multiple organs, especially muscle tissue. Organs with higher blood volume excrete the ions quickly; however, organs with lower blood supply retain the ions for longer periods of time which can also buildup over time known as bioaccumulation. The most common place to find K and Cs in the ocean is in the muscle of fish. Due to the intake of Cs into fish in place of K, it is important to look at K concentration effects on adsorption (Whaley, 1973). There are small fluctuations as concentration increases; however, an overall trend of declining adsorption with increasing concentration is seen. The variation is minimal when reflecting on the uncertainties seen for each concentration. Similar fluctuations and uncertainties are seen in all of the competing ion experiments. Despite the decrease of adsorption of Cs as concentration increased, adsorption did not fall below 98% with the lowest adsorption at a concentration of 1.0 M showing little competition with Cs-137.

5.4 NaCl Study

Similarly to the KCl study, NaCl was studied to observe any effects on adsorption of Cs in water samples. Na is also a Group 1A element and is a component of ocean water. Similar

fluctuations with increasing concentration that were seen in the KCl study were also seen in the NaCl study, but to a smaller degree. The main increase in Cs adsorption before a steady decrease in adsorption is seen from a concentration of 0.1 M to 0.25 M which is seen in all of the competing ion studies. The lowest adsorption was 98% at 0.1 M concentration. A trend was also seen with decreasing adsorption with increased concentrations. Despite the decrease, high adsorption rates showed little competition with Na and Cs-137. The study is important due to the salinity of the ocean, which is made up of mainly NaCl.

5.5 RbCl Study

Rb is also a Group 1A element in the periodic table with a plus one charge. Though Rb is not as common in ocean water, Rb was included as it was a Group 1A element and has a similar ionic size to that of Cs with Rb measuring 0.15 nm and Cs measuring 0.17 nm (Whaley, 1973). The similarity in size and charge was theorized to make Rb an excellent competing ion example which is further seen in the results of the study. Similar fluctuations were seen with increasing concentration with further decrease as concentration increased. Compared to the other competing ions, Rb had the lowest adsorption rates with a low of around 68% at 1.0 M concentration. The study helped to show that Cs binds to the Prussian Blue coating by switching places with the K in the voids of the lattice matrix. The Rb is more favorable for binding than the Cs or K which explains the lower adsorption seen in the study (Whaley, 1973).

5.6 LiCl Study

As with the other salt studies, Li was studied due to being a Group 1A element with a plus one chage. Fluctuations were also seen with increasing concentrations with a lowest adsorption of around 97% at 1.0 M concentration. The ionic size of Li is 0.068 nm which is

significantly smaller than that of Cs. The smaller size could play a factor in lower adsorption rates than that of KCl and NaCl. LiCl also has a high charge density which could factor into being more favorable when binding to the DND (William, 1973). Though LiCl has a higher ionic size and charge density, only RbCl saw a significant decrease in adsorption of Cs from water samples with LiCl coming in a close second. LiCl has a higher affinity for water and disperses more readily in water which would explain why the adsorption, though lower than the NaCl and KCl, was not lower than the RbCl, which was more favorable to binding with the PB coated DND.

Element	Concentration in Ocean (parts per million) (ppm)	Range of Concentrations Tested	Ionic Size (nm)	Slope of Model for Adsorption	R2 for Adsorption Model	Average Adsorption in % across model
Li	0.1-0.2	0.001 mL to 1.0 mL	0.068	-1.1339	0.3486	99.09%
Na	10,561	0.001 mL to 1.0 mL	0.095	-0.1108	0.0085	99.43%
K	380	0.001 mL to 1.0 mL	0.133	-0.3035	0.0641	99.19%
Rb	0.120	0.001 mL to 1.0 mL	0.148	-23.663	0.8047	92.21%
Cs	0.002	0.1 mL (1 Bq)	0.169	N/a	N/a	N/a

Table 1 shows the concentration of each competing ion in ocean water compared to Cs in ocean water. The experimental range is listed to demonstrate the large range observed compared to real concentrations. A list of each competing ions iconic size is also listed to further the understanding of competition among the ions (Whaley, 1973). The R2 values show no statistical correlation between the data points.

5.7 Stable Cs Study

The HPGe detector used has previously had difficulty detecting low levels of Cs-137 with an activity of 1 Bq (0.001 mL). It was theorized that adding stable Cs to the samples would increase the adsorption and detection of Cs-137. Various amounts of stable Cs were added to the samples ranging from 0.01 μg to 10 μg. Despite the added stable Cs, the HPGe detector continued having difficulty in detecting low levels of Cs-137 which shows in the large range of adsorptions and high uncertainties seen in Graph 7. Adsorption varied significantly throughout the range with the lowest being around 61% at 0.05 μg stable Cs in 9.994 mL DI and the highest being around 137% at 2.5 μg stable Cs. The uncertainties were large and ranged from 8.04 to 49.40.

BIBLIOGRAPHY

1. Babenya Julia S; Kazakov Andrey G; Ekatova Taisya Y; Yakovlev Rusian Y. "The dependence of ^{90}Y sorption on nanodiamonds on sizes of their aggregates in water solutions", *Journal of Radioanalytical and Nuclear Chemistry,* (2021), 1027-1030.
2. Baum E; Ernesti M; et al. "Nuclides and Isotopes, Chart of Nuclides, Seventeenth Edition". *KAPL,* 2010.
3. Deak A. "Study of hexacyanoferrate(II) nanodiamond absorbent for the preconcentration of cesium and size categorization of radiocesium particles from contaminated soils", M.S. Thesis, *Colorado State University*, (2021).
4. Elder T. "Wood: Chemically Modified." *Journal of Molecular Liquids.* (2001), 1.
5. Fifield F. W. "Principles and Practice of Analytical Chemistry." *Blackwell Science. University of Surrey.* (2000). 37-49.
6. IAEA. "IAEA Comprehensive Report on the Safety Review of the ALPS-Treated Water at the Fukushima Daiichi Nuclear Power Station." *IAEA.* (2023). 33-111.
7. Jundong Feng; Xida Zhao; Hao Zhou; Liang Qiu; Yaodong Dai; Hulyao Luo; Marta Otero. "Removal of strontium by high-performance adsorbents Saccharomyces cerevisiae-Fe_3O_4 bio-microcomposites", *Journal of Radioanalytical and Nuclear Chemistry,* (2020), 525-535.
8. Jung-Weon Choi; Yoon-Ji Park; Hyun-Kyu Lee; Sang-June Choi. "Amine-Functionalized graphene oxide/zinc hexacyanoferrate composites for cesium removal from aqueous solutions", *Journal of Radioanalytical and Nuclear Chemistry*, (2020), 785-792.

9. Kharisov Boris I; Kharissova Oxana V; Chavez-Guerrero Leonardo. “Synthesis Techniques, Properties, and Applications of Nanodiamonds”, *Taylor and Francis Group,* (2010), 84-96.
10. Komal Kashyap; Fahmida Khan; Dakeshwar Kumar Verma; Sonalika Agrawal. “Effective removal of uranium from aqueous solution by using cerium oxide nanoparticles derived from citrus limon peel extract”, *Journal of Radioanalytical and Nuclear Chemistry,* (2021), 1-11.
11. Labib Sh; Shahr El-Din A.M; K.F Allan; M.F Attallah. “Synthesis of highly deficient nano $SrCoO_x$ for the purification of lanthanides from monazite concentrate”, *Journal of Radioanalytical and Nuclear Chemistry*, (2020), 1179-1187. 1-14.
12. Matsumoto K; Yamato H; Kakimoto S; Yamashita T; Wada R; Tanaka Y; Akita M; Fukimura T. “A Highly Efficient Adsorbent Cu-Perusian Blue @ Nanodiamond for Cesium in Diluted Artificial Seawater and Soil-Treated Wastewater.” *Scientific Reports,* (2018).
13. Meiqing Fan; Xiao’e Wang; Qiong Song; Liying Zhang; Bo Ren; Xiaodong Yang. “Review of biomass-based materials for uranium adsorption”, *Journal of Radioanalytical and Nuclear Chemistry,* (2021), 589-598.
14. Schrand Amanda M; Ciftan Hens Suzanne A; Schenderova Olga A. “Nanodiamond Particles: Properties and Perspectives for Bioapplications”, *Critical Reviews in Solid State and Materials Sciences,* (2009), 18-62.
15. Whaley T. “Sodium, Potassium, Rubidium, Cesium, and Francium”. *Pergamon Press*, (1973), 409-410.
16. William A. Hart O.F. Beumal Jr. “The Chemistry of Lithium”. *Pergamon Press*, (1973), 340-348.

17. World Ocean Review. “Water a Unique Molecule.” *https://worldoceanreview.com/en/wor-1/climate-system/great-ocean-currents/water-a-unique-molecule/.*

18. Yang Li; Houjun He; Zuocong Liu; Zeen Lai; Yun Wang. “A facile method for preparing three-dimensional graphene nanoribbons aerogel for uranium (VI) and thorium (IV) adsorption”, *Journal of Radioanalytical and Nuclear Chemistry*, (2021), 289-297.

Appendix I: Raw Data

Table 2: pH Study

Sample	Time (hr)	Counts	Background Corrected Counts	Nuclide area	Energy (keV)	Activity (Bq)	Percent	Average
blank	6	11	0	38 +- 70.28%	662.0	N/a	N/a	N/a
Cs no DND	6	5709	5698	38140 +- 0.52%	661.7	440.22	N/a	N/a
pH 3.0	6	50	39	131 +- 24.75%	661.7	1.51	99.66%	
pH 3.0	6	40	29	143 +- 20.54%	661.7	1.65	99.63%	
pH 3.0	6	38	27	45 +- 66.82%	661.7	0.52	99.88%	99.72%
pH 3.5	6	41	30	124 +- 25.12%	661.7	1.43	99.68%	
pH 3.5	6	43	32	34 +- 85.12%	661.7	0.39	99.91%	
pH 3.5	6	40	29	90 +- 34.29%	661.7	1.04	99.76%	99.78%
pH 4.0 (1)	6	45	34	59 +- 5.17%	661.7	0.68	99.85	
pH 4.0 (2)	6	42	31	2 +- 1384.79%	661.7	0.02	99.99	
pH 4.0 (3)	6	30	19	20 +- 156.59%	661.7	0.23	99.95	99.93%
pH 4.5 (1)	6	71	60	340 +- 9.86%	661.7	3.92	99.11	
pH 4.5 (2)	6	71	60	269 +- 12.09%	661.7	3.10	99.29	
pH 4.5 (3)	6	76	65	262 +- 13.07%	661.7	3.02	99.31	99.24%
pH 5.0 (1)	6	51	40	150 +- 3.20%	661.7	1.73	99.61	
pH 5.0 (2)	6	80	69	211 +- 16.40%	661.7	2.44	99.45	
pH 5.0 (3)	6	132	121	507 +- 7.61%	661.7	5.85	98.67	99.24%
pH 5.5 (1)	6	60	49	164 +- 19.93%	661.7	1.89	99.57	
pH 5.5 (2)	6	47	36	35 +- 91.29%	661.7	0.40	99.91	99.68%

pH 5.5 (3)	6	47	36	164 +- 19.18%	661.7	1.89	99.57	
pH 6.0 (1)	6	51	40	184 +- 18.41%	661.7	2.12	99.52	
pH 6.0 (2)	6	44	33	240 +- 13.33%	661.7	2.77	99.37	
pH 6.0 (3)	6	89	78	512 +- 6.83%	661.7	5.91	98.66	99.18%
pH 6.5 (1)	6	233	222	1381 +- 3.44%	661.7	15.94	96.38%	
pH 6.5 (2)	6	399	388	2624+- 2.25%	661.7	30.29	93.12%	
pH 6.5 (3)	6	262	251	1712 +- 2.95%	661.7	19.76	95.51%	95.00%
pH 7.0 (1)	6	174	163	1054 +- 4.17%	662.0	12.17	97.17%	
pH 7.0 (2)	6	255	244	1602 +- 3.07%	661.7	18.49	95.73%	
pH 7.0 (3)	6	287	276	1739 +- 2.96%	661.7	20.07	95.37%	96.09%
pH 7.5 (1)	6	270	259	1818 +- 2.74%	661.7	20.98	95.23%	
pH 7.5 (2)	6	97	86	474 +- 7.94%	661.7	5.47	98.76%	
pH 7.5 (3)	6	213	202	1317 +- 3.57%	661.7	15.20	96.55%	96.85%
pH 8.0 (1)	6	313	302	1911 +- 2.79%	661.7	22.06	94.99%	
pH 8.0 (2)	6	161	150	918 +- 4.59%	661.7	10.60	97.59%	
pH 8.0 (3)	6	259	248	1351 +- 3.48%	661.7	15.59	96.46%	96.35%
pH 8.5 (1)	6	241	230	1382 +- 3.48%	661.7	15.94	96.38%	
pH 8.5 (2)	6	233	222	1453 +- 3.31%	661.7	16.77	96.19%	
pH 8.5 (3)	6	334	323	2053 +- 2.64%	661.7	23.70	94.62%	95.73%
pH 9.0 (1)	6	136	125	593 +- 6.45%	661.7	6.84	98.45%	
pH 9.0 (2)	6	276	265	1647 +- 2.71%	661.7	19.01	95.68%	
pH 9.0 (3)	6	352	341	2075 +- 2.35%	661.7	23.95	94.56%	96.23%

Table 3: Temperature Study

Sample	Time (hr)	Counts	Background Corrected Counts	Nuclide area	Energy (keV)	Activity (Bq)	Percent	Average
blank	6	11	0	38 +- 70.28%	662.0	N/a	N/a	N/a
Cs no DND	6	5709	5698	38140 +- 0.52%	661.7	440.22	N/a	N/a
4°C	6	115	104	678 +- 4.73%	661.7	7.83	98.22	
4°C	6	74	63	271 +- 12.84%	661.7	3.13	99.29	
4°C	6	80	69	384 +- 6.74%	661.7	4.43	98.99	98.83
10°C	6	103	92	459 +- 6.34%	661.7	5.30	98.8	
10°C	6	55	44	149 +- 21.64%	661.7	1.72	99.61	
10°C	6	41	30	62 +- 131.21%	661.7	0.72	99.84	99.42
15°C	6	95	84	463 +- 6.06%	661.7	5.34	98.79	
15°C	6	54	43	182 +- 17.68%	661.7	2.10	99.52	
15°C	6	58	47	181 +- 18.69%	661.7	2.09	99.53	99.28
20°C	6	114	103	468 +- 6.51%	661.7	5.40	98.77	
20°C	6	64	53	307 +- 10.94%	661.7	3.54	99.20	
20°C	6	73	62	253 +- 9.76%	661.7	2.92	99.34	99.10
25°C	6	85	74	391 +- 6.85%	661.7	4.51	98.98	
25°C	6	58	47	180 +- 12.06%	661.7	2.08	99.53	
25°C	6	46	35	154 +- 14.85%	661.7	1.78	99.60	99.70
30°C	6	70	59	176 +- 13.83%	661.7	2.03	99.54	
30°C	6	59	48	187 +- 12.41%	661.7	2.16	99.51	
30°C	6	57	46	154 +- 14.49%	661.7	1.78	99.60	99.55

35°C	6	25	14	74 +- 27.27%	661.7	0.85	99.81	
35°C	6	37	26	58 +- 37.54%	661.7	0.67	99.85	
35°C	6	73	62	286 +- 8.78%	661.7	3.30	99.25	99.64
40°C	6	39	28	106 +- 19.54%	661.7	1.22	99.72	
40°C	6	33	22	15 +- 133.82%	661.7	0.17	99.96	
40°C	6	57	46	158 +- 14.82%	661.7	1.82	99.59	99.76
45°C	6	80	69	373 +- 7.58%	661.7	4.31	99.02	
45°C	6	39	28	88 +- 24.00%	661.7	1.02	99.77	
45°C	6	45	34	138 +- 16.02%	661.7	1.59	99.64	99.48
50°C	6	44	33	123 +- 17.73%	661.7	1.42	99.68	
50°C	6	35	24	60 +- 34.47%	661.7	0.69	99.84	
50°C	6	66	55	411 +- 6.64%	661.7	4.74	98.92	99.48

Table 4: Competing Ion Study (KCl)

Sample	Time (hr)	Counts	Background Corrected Counts	Nuclide area	Energy (keV)	Activity (Bq)	Percent	Average
blank	6	11	0	38 +- 70.28%	662.0	N/a	N/a	N/a
Cs no DND	6	5709	5698	38140 +- 0.52%	661.7	440.22	N/a	N/a
0.001 M	6	50	39	90 +- 34.14%	661.7	1.04	99.76	
0.001 M	6	38	27	124 +- 16.46%	661.7	1.43	99.68	
0.001 M	6	57	46	242 +- 13.87%	661.7	2.79	99.37	99.60%
0.005 M	6	63	52	209 +- 16.01%	661.7	2.41	99.45	99.33%

0.005 M	6	79	68	383 +- 6.96%	661.7	4.42	99.00	
0.005 M	6	88	77	177 +- 12.29%	661.7	2.04	99.54	
0.01 M	6	55	44	204 +- 16.50%	661.7	2.35	99.47	
0.01 M	6	78	67	351 +- 7.56%	661.7	4.05	99.08	
0.01 M	6	181	170	908 +- 3.87%	661.7	10.48	97.62	98.72%
0.05 M	6	49	38	209 +- 16.01%	661.7	2.41	99.45	
0.05 M	6	81	70	383 +- 6.96%	661.7	4.42	99.00	
0.05 M	6	42	31	177 +- 12.29%	661.7	2.04	99.54	99.33%
0.1 M	6	83	72	343 +- 10.24%	661.7	3.96	99.10	
0.1 M	6	119	108	551 +- 6.95%	661.7	6.36	98.56	
0.1 M	6	85	74	375 +- 9.61%	661.7	4.33	99.02	98.89%
0.25 M	6	55	44	167 +- 13.36%	661.7	1.93	99.56	
0.25 M	6	40	29	58 +- 53.91%	661.7	0.67	99.85	
0.25 M	6	55	44	206 +- 15.51%	661.7	2.38	99.46	99.62%
0.5 M	6	60	49	247 +- 9.18%	661.7	2.85	99.35	
0.5 M	6	120	109	221 +- 10.39%	661.7	2.55	99.42	
0.5 M	6	97	86	210 +- 15.94%	661.7	2.42	99.45	99.41%
1M	6	89	78	338 +- 10.37%	661.7	3.9	99.11	
1M	6	109	98	539 +- 6.89%	661.7	6.22	98.59	
1M	6	112	101	708 +- 5.51%	661.7	8.17	98.14	98.61%

Table 5: Competing Ion Study (NaCl)

sample	time (hr)	Counts	Background Corrected Counts	Nuclide area	Energy (keV)	Activity (Bq)	Percent	Average
blank	6	11	0	38 +- 70.28%	662.0	N/a	N/a	N/a
Cs no DND	6	5709	5698	38140 +- 0.52%	661.7	440.22	N/a	N/a
0.001 M	6	43	32	146 +- 21.73%	661.7	1.69	99.62	
0.001 M	6	30	19	72 +- 27.07%	661.7	0.83	99.81	
0.001 M	6	61	50	263 +- 8.59%	661.7	3.04	99.31	99.58%
0.005 M	6	51	40	176 +- 12.43%	661.7	2.03	99.54	
0.005 M	6	37	26	55 +- 58.48%	661.7	0.63	99.86	
0.005 M	6	57	46	221 +- 10.59%	661.7	2.55	99.42	99.61%
0.01 M	6	44	33	85 +- 37.11 %	661.7	0.98	99.78	
0.01 M	6	37	26	60 +- 33.90%	661.7	0.69	99.84	
0.01 M	6	49	38	134 +- 16.54%	661.7	1.55	99.65	99.76%
0.05 M	6	62	51	160 +- 19.69%	661.7	1.85	99.58	
0.05 M	6	48	37	70 +- 43.24%	661.7	0.81	99.82	
0.05 M	6	62	51	237 +- 14.17%	661.7	2.74	99.38	99.59%
0.1 M	6	100	89	584 +- 5.26%	661.7	6.71	98.48	
0.1 M	6	79	68	402 +- 6.60%	661.7	4.64	98.95	
0.1 M	6	79	68	525 +- 6.80%	661.7	6.06	98.62	98.68%
0.25 M	6	36	25	123 +- 17.48%	661.7	1.42	99.68	
0.25 M	6	38	27	121 +- 16.18%	661.7	1.40	99.68	
0.25 M	6	58	47	245 +- 9.21%	661.7	2.83	99.36	99.57%

0.5 M	6	64	53	239 +- 9.89%	661.7	2.76	99.37	
0.5 M	6	43	32	102 +- 31.01%	661.7	1.18	99.73	
0.5 M	6	78	67	308 +- 8.265	661.7	3.56	99.19	99.43%
1M	6	66	55	315 +- 7.82%	661.7	3.64	99.17	
1M	6	76	65	249 +- 11.19%	661.7	2.87	99.35	
1M	6	78	67	361 +- 7.49%	661.7	4.17	99.05	99.19%

Table 6: Competing Ion Study (RbCl)

sample	time (hr)	Counts	Background Corrected Counts	Nuclide area	Energy (keV)	Activity (Bq)	Percent	Average
blank	6	11	0	38 +- 70.28%	662.0	N/a	N/a	N/a
Cs no DND	6	5709	5698	38140 +- 0.52%	661.7	440.22	N/a	N/a
0.001 M	6	272	261	1385 +- 2.97%	661.7	15.99	96.37	
0.001 M	6	171	160	948 +- 3.72%	661.7	10.94	97.51	
0.001 M	6	184	173	1617 +- 3.10%	661.7	18.66	95.76	96.55%
0.005 M	6	140	129	905 +- 3.90%	661.7	10.45	97.63	
0.005 M	6	218	207	1232 +- 3.24%	661.7	14.22	96.77	
0.005 M	6	150	139	883 +- 4.70%	661.7	10.19	97.68	97.36%
0.01 M	6	182	171	1124 +- 3.40%	661.7	12.97	97.05	
0.01 M	6	224	213	1160 +- 3.31%	661.7	13.39	96.96	
0.01 M	6	197	186	1114 +- 3.41%	661.7	12.86	97.08	97.03%
0.05 M	6	160	149	1105 +- 3.38%	661.7	12.75	97.10	97.59%

0.05 M	6	149	138	880 +- 4.72%	661.7	10.16	97.69	
0.05 M	6	140	129	773 +- 5.30%	661.7	8.92	97.97	
0.1 M	6	469	458	3523 +- 1.77%	661.7	40.66	90.76	
0.1 M	6	457	446	3480 +- 1.80%	661.7	40.17	90.88	
0.1 M	6	490	479	3476 +- 1.78%	661.7	40.12	90.89	90.84%
0.25 M	6	315	304	2311 +- 2.23%	661.7	26.67	93.94	
0.25 M	6	357	346	2369 +- 2.44%	661.7	27.34	93.79	
0.25 M	6	262	251	2361 +- 2.20%	661.7	27.25	93.81	93.85%
0.5 M	6	361	350	2247 +- 2.24%	661.7	25.94	94.11	
0.5 M	6	372	361	2357 +- 2.40%	661.7	27.21	93.82	
0.5 M	6	237	226	1712 +- 2.66%	661.7	19.76	95.51	94.48%
1M	6	1690	1679	11386 +- 0.97%	661.7	131.42	70.15	
1M	6	1728	1717	11526 +- 0.91%	661.7	132.98	69.79	
1M	6	1565	1554	11480 +- 0.97%	661.7	132.51	69.90	69.95%

Table 7: Competing Ion Study (LiCl)

Sample	Time (hr)	Counts	Background Corrected Counts	Nuclide area	Energy (keV)	Activity (Bq)	Percent	Average
blank	6	11	0	38 +- 70.28%	662.0	N/a	N/a	N/a
Cs no DND	6	5709	5698	38140 +- 0.52%	661.7	440.22	N/a	N/a

0.001 M	6	49	38	249 +- 9.32%	661.7	2.87	99.35	
0.001 M	6	98	87	523 +- 7.32%	661.7	6.04	98.63	
0.001 M	6	107	96	482 +- 7.88%	661.7	5.56	98.74	98.91%
0.005 M	6	113	102	575 +- 5.32%	661.7	6.64	98.49	
0.005 M	6	127	116	871 +- 3.92%	661.7	10.05	97.72	
0.005 M	6	62	51	191 +- 17.86%	661.7	2.20	99.50	98.57%
0.01 M	6	56	45	199 +- 11.28%	661.7	2.30	99.48	
0.01 M	6	37	26	96 +- 21.20%	661.7	1.11	99.75	
0.01 M	6	56	45	150 +- 21.73%	661.7	1.73	99.61	99.61%
0.05 M	6	37	26	145 +- 14.36%	661.7	1.67	99.62	
0.05 M	6	47	36	186 +- 16.78%	661.7	2.15	99.51	
0.05 M	6	70	59	265 +- 9.12%	661.7	3.06	99.31	99.48%
0.1 M	6	50	39	140 +- 14.50%	661.7	1.62	99.63	
0.1 M	6	39	28	174 +- 12.54%	661.7	2.01	99.54	
0.1 M	6	43	32	181 +- 11.66 %	661.7	2.09	99.53	99.57%
0.25 M	6	47	36	210 +- 10.55%	661.7	2.42	99.45	
0.25 M	6	45	34	187 +- 12.35%	661.7	2.16	99.51	
0.25 M	6	82	71	509 +- 7.26%	661.7	5.88	98.67	99.21%
0.5 M	6	48	37	155 +- 14.59%	661.7	1.79	99.59	
0.5 M	6	43	32	62 +- 49.06%	661.7	0.72	99.84	
0.5 M	6	47	36	144 +- 14.24%	661.7	1.66	99.62	99.68%
1M	6	223	212	1246 +- 3.15%	661.7	14.38	96.73	97.72%
1M	6	122	111	782 +- 4.30%	661.7	9.03	97.95	

1M	6	99	88	579 +- 6.43%	661.7	6.68	98.48	

Table 8: Stable Cs Study

Sample (µg)	Counts	Background Corrected Counts	Area	Error	Activity	Adsorption	Average Adsorption	Uncertainty
Blank	5	0						
Cs no DND	23	18						
	28	23	43	68.42%	0.50	85.57		
	29	24	57	56.08%	0.66	113.43		
	19	14	37	48.66%	0.43	73.63		
	15	10	8	231.05%	0.09	15.92		
	27	22	54	53.64%	0.62	107.46		
	28	23	90	53.64%	1.00	179.10		
0.01	36	31	125	25.59%	1.44	248.76	79.20	38.88
	27	22	47	37.32%	0.54	93.53		
	38	33	73	25.85%	0.84	145.27		
	20	15	5	582.16%	0.06	9.95		
	20	15	5	389.27%	0.06	9.95		
	30	25	42	44.57%	0.48	83.58		
	18	13	28	105.28%	0.32	55.72		
0.05	30	25	17	105.50%	0.20	33.83	61.69	49.40
	30	25	53	34.69%	0.61	105.47		
	17	12	15	122.64%	0.17	29.85		
	31	26	43	43.54%	0.50	85.57		
	24	19	36	53.07%	0.42	71.64		
0.1	57	52	353	9.57%	4.07	702.49	73.13	32.02
	42	37	114	17.02%	1.32	226.87		
	27	22	69	28.04%	0.80	137.31		
	34	29	73	26.53%	0.84	145.27		
	39	34	47	64.07%	0.54	93.53		
	34	29	72	28.01%	0.83	143.28		
	20	15	50	36.04%	0.58	99.50		
0.5	18	13	51	34.63%	0.59	101.49	120.06	24.26
	30	25	45	41.55%	0.52	89.55		
	20	15	55	33.46%	0.63	109.45		
1,0	28	23	21	140.22%	0.24	41.79	85.90	41.46

	25	20	52	56.50%	0.60	103.48		
	37	32	70	42.59%	0.81	139.30		
	26	21	16	111.82%	0.18	31.84		
	457	452	1163	3.89%	13.42	2315.43		
	32	27	71	27.27%	0.82	141.29		
	27	22	117	25.59%	1.35	232.84		
	37	32	78	41.51%	0.90	155.22		
	26	21	47	40.17%	0.54	93.53		
	35	30	80	35.82%	0.92	159.20		
2.5	41	36	104	18.81%	1.20	206.97	137.31	30.18
	27	22	32	55.73%	0.37	63.68		
	29	24	29	61.26%	0.33	57.71		
	31	26	37	48.66%	0.43	73.63		
5.0	106	101	616	6.21%	7.11	1225.87	65.01	8.04
	29	24	34	54.34%	0.39	67.66		
	122	117	582	6.29%	6.72	1164.18		
	35	30	72	24.69%	0.83	143.28		
	29	24	33	92.35%	0.38	65.67		
	46	41	80	38.21%	0.92	159.20		
10	32	27	38	74.77%	0.44	75.62	102.29	45.20

Appendix II: HPGe Gamma Spectrum

Spectrum 1: Before Background Correction

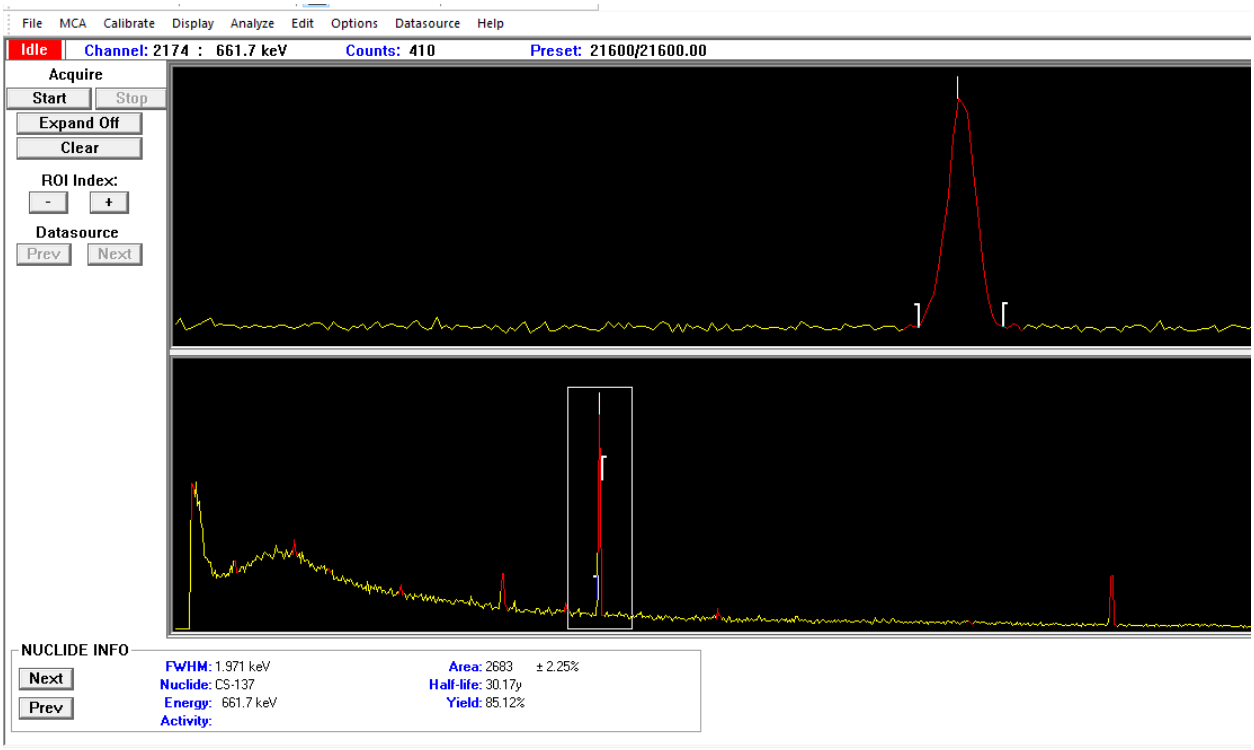

Spectrum 2: Background Corrected

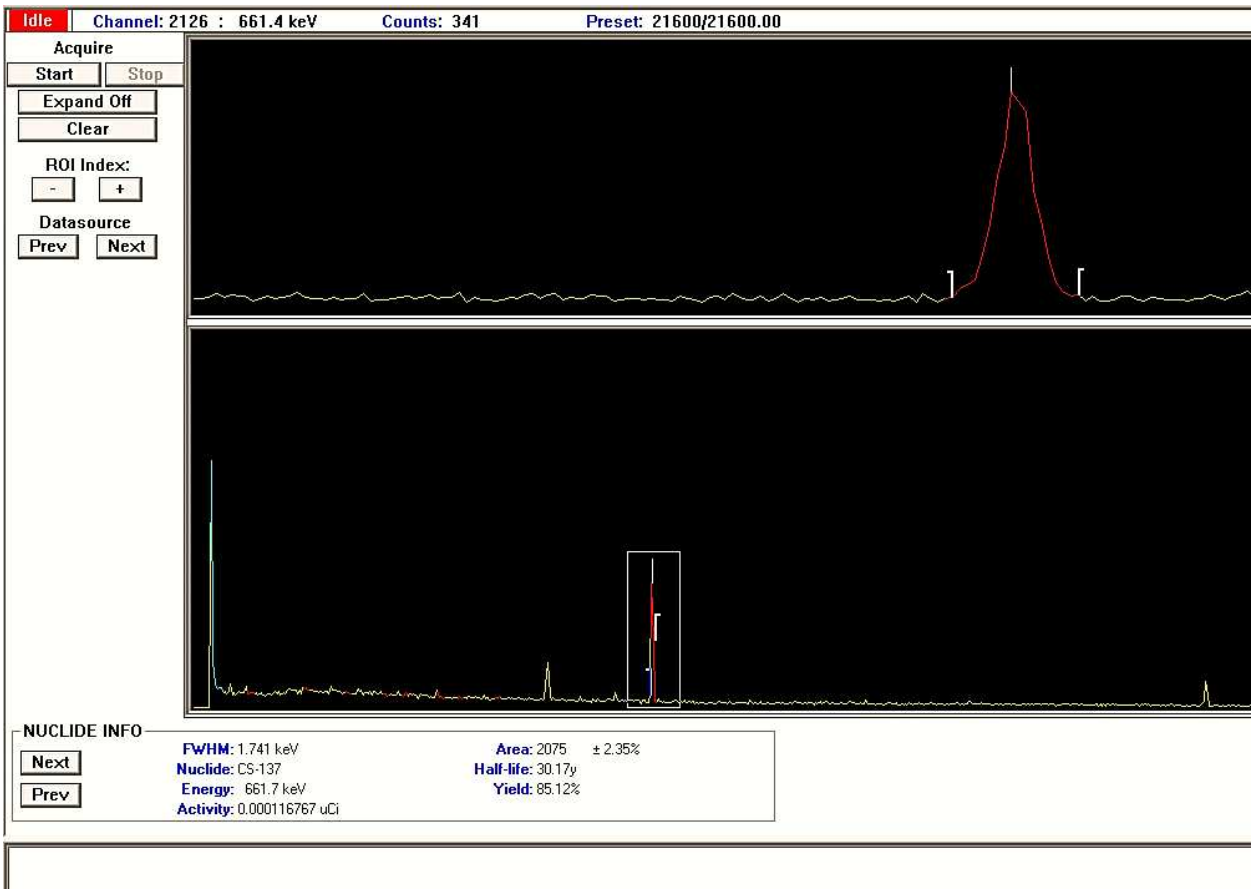

Appendix III: Equations

$$\text{Activity} = \frac{Area}{efficiency\ x\ branching\ ratio\ x\ time\ (s)}$$

$$\text{Percent Adsorbed} = \frac{100\%}{Activity\ of\ stock\ solution}\ x\ (Activity\ of\ stock\ solution - Activity\ of\ sample)$$

All standard deviations were calculated in Excel using the formula =STDEV(G#:G#).